Int. J. Heat Mass Transfer. Vol. 35, No. 7, pp. 1681–1694, 1992
Printed in Great Britain

0017 9310/92 $5.00 + 0.00

Frozen start-up behavior of low-temperature heat pipes

AMIR FAGHRI

Brage Golding Distinguished Professor, Department of Mechanical and Materials Engineering, Wright State University, Dayton, OH 45435, U.S.A.

(*Received* 7 *March* 1991 *and in final form* 24 *June* 1991)

Abstract—Start-up and subsequent operation of a low-temperature heat pipe requires the liquid phase of the operating fluid to be continuously pumped back to the evaporator by the capillary action of the wick. If the pipe has been in an environment where ambient temperatures are below the freezing point of the working fluid prior to start-up, the frozen fluid in the condenser and adiabatic regions can prevent initial flow to the evaporator, causing dryout of the evaporator before all of the working fluid is in the liquid phase. This paper examines the time-dependent wall and vapor temperature profiles along the axial length of a low-temperature heat pipe during start-up from the frozen state, and freeze-out during normal operation by applying a subfreezing temperature fluid through the condenser. In addition, the experimental transient frozen start-up wall temperature profile is compared with a two-dimensional numerical phase-change model. A successful start-up method using a pulsed power input is presented.

INTRODUCTION

LOW- TO medium-temperature heat pipes are presently used in a number of applications from electronics cooling to waste heat recovery. One of the limiting factors in the heat pipe design is the start-up environment. If the temperature of the environment is below the freezing temperature of the working fluid, start-up can be difficult if not impossible. Most of the experiments performed on heat pipes to date have been aimed at finding the maximum heat transfer, maximum temperature environments, best working fluids and optimal wick structures. Very few studies have examined the frozen start-up behavior of low- and medium-temperature heat pipes. Also, these previous studies are generally incomplete in nature.

A low-temperature stainless steel/water heat pipe was started from the frozen state by Neal [1]. No special stepwise introduction of heat load to the evaporator was attempted and the heat pipe did not reach any meaningful operating condition prior to the evaporator drying out. Neal also attempted start-up with only the condenser frozen and experienced dryout after 20 min of operation. However, no time-dependent data were recorded, such as wall or vapor temperatures.

In a similar experiment, Deverall and Kemme [2] experienced immediate dryout in a low-temperature heat pipe with a heat input of only 10 W. Some success, however, was realized by the injection of a small amount of noncondensable gases within the heat pipe prior to freezing, which blocked a significant portion of the condenser section, thus allowing a gradual start-up. Again, no time-dependent temperature data were available.

Time-dependent data are available for the frontal start-up of high-temperature heat pipes using liquid-metal working fluids (e.g. Cotter *et al.* [3]). Although the high-temperature heat pipe experiments are similar in that they involve the phase change of working fluid from solid to liquid, there is a great deal of difference in the relative operating temperature and frozen start-up behavior compared to a low-temperature pipe.

In an effort to obtain information on the phenomena of frozen start-up, a simple copper/water heat pipe was tested under the following five conditions.

(a) The entire heat pipe was frozen to approximately $-21°C$ with a subsequent start-up attempt while monitoring the vapor and wall temperatures along the pipe. The heat pipe remained in the freezer throughout this test.

(b) Same as (a) only the heat heat pipe was removed from the freezer before start-up was attempted. Ambient temperatures were approximately 21°C during this test.

(c) The heat pipe was frozen at room temperature using a chiller, which supplied $-15°C$ ethylene glycol to the condenser. Start-up was attempted after the entire pipe was frozen.

(d) After the heat pipe was operating under steady-state conditions (normal start-up procedure used), the condenser was frozen using $-15°C$ ethylene glycol.

(e) Same procedure as (b) but heat was applied in pulses. Pulse criteria were based on earlier experimental data gathered.

Throughout all of the experiments, data were also taken during the freezing process, i.e. the change of phase from liquid to solid prior to the start-up attempt. This ensured that the fluid in the heat pipe

NOMENCLATURE

c_p	specific heat at constant pressure [J kg^{-1} K^{-1}]
H_{sl}	latent heat of melting per unit volume [J m^{-3}]
K	thermal conductivity [W m^{-1} K^{-1}]
n	outward normal direction
r	radial coordinate
S	interface position vector [m]
t	time [s]
T	temperature [K]
T_m	melting temperature [K]
T_0	initial temperature [K]
V	volume [m^3]
x	axial coordinate.

Greek symbols

$\delta(T-T_m)$	Dirac function
ΔT	small finite temperature interval around T_m to define mushy zone [K]
ε	porosity
ρ	density [kg m^{-3}].

Subscripts

cc	copper clamp
ck	cork
fl	working substance in the liquid state in the wick
fs	working substance in the solid state in the wick
h	heater
le	wick region where the working substance is in the liquid state
me	wick region where the working substance is in the mushy state
s	wick structure material
sc	wick region where the working substance is in the solid state
w	properties at the heat pipe wall.

had completely changed to the solid phase before each start-up attempt.

The objectives for the present study are as follows:

(a) obtain time-dependent wall and vapor temperature profiles along the heat pipe;

(b) suggest procedures for successful start-up from the frozen state for low-temperature heat pipes; and

(c) provide an accurate numerical simulation model of the melting process which will aid in the prediction of start-up failure due to the frozen working fluid.

EXPERIMENTAL SET-UP AND PROCEDURE

Figure 1 is a schematic of the experimental set-up used in the present study. Seventeen Type K thermocouples with uncertainties of ± 0.5°C were mounted on the outer wall along the pipe and a multi-point Type K thermocouple probe with six thermocouple beads was inserted into the vapor space along the pipe axis. The axial locations of all thermocouples are shown in Fig. 2. All temperatures were monitored and recorded by a Fluke 2285B Datalogger with Prologger software at 30 s intervals. Three flexible, etched-foil heaters rated at 235 W each were installed side-by-side on the pipe, wired in parallel, and controlled by a single variable a.c. transformer. The voltage and amperage delivered to the heaters were measured directly with a multimeter to determine the total power input. The heaters were mounted to the heat pipe by first surrounding them with a thin layer of cork. A copper pipe with inside diameter slightly smaller than the cork-covered evaporator was split down the axis to provide two halves of a clamp to compress the heaters onto the pipe. The cork assured uniform clamping pressure over the entire heater surface. The annular condenser was cooled with a Neslab RTE-4 chiller, which used ethylene glycol as the coolant fluid. It was critical that the heat pipe be maintained in an absolutely horizontal position during all tests to avoid a liquid pool at either end of the heat pipe. For this reason, the heat pipe was mounted on an optical bench and adjusted to horizontal with a precision spirit level. The following is a description of the heat pipe itself. The container and wick were copper. The outer and inner diameters of the pipe were 25.4 and 22.0 mm, respectively. The wick was made of a screen mesh with wire diameter of 0.178 mm, thickness 0.356 mm, and mesh number 1.97×10^3 m^{-1}. Two wraps of the screen mesh resulted in a vapor space diameter of 20.5 mm. The heat pipe was cleaned using standard procedures and filled with 40 cm^3 of distilled water. The entire heat pipe assembly was insulated with 50 mm of tightly-wrapped Fiberfrax ceramic wool insulation.

A baseline experiment was performed on the heat pipe for time-dependent wall and vapor temperature data during normal start-up, where the working fluid was in the liquid state. This test was performed with the same experimental set-up and heat input as the frozen-state start-up attempts for a valid comparison. Since no other frozen start-up profile was available for comparison, a suitable criterion for evaluating when the heat pipe had actually begun to dry out was needed. A group of preliminary experiments was used to obtain this criterion. Based on these early experiments and the baseline run, it was determined that the onset of dryout occurred when the temperature difference between any two vapor temperatures exceeded 3°C. To prevent damage to the heaters, testing was discontinued when heater temperatures were

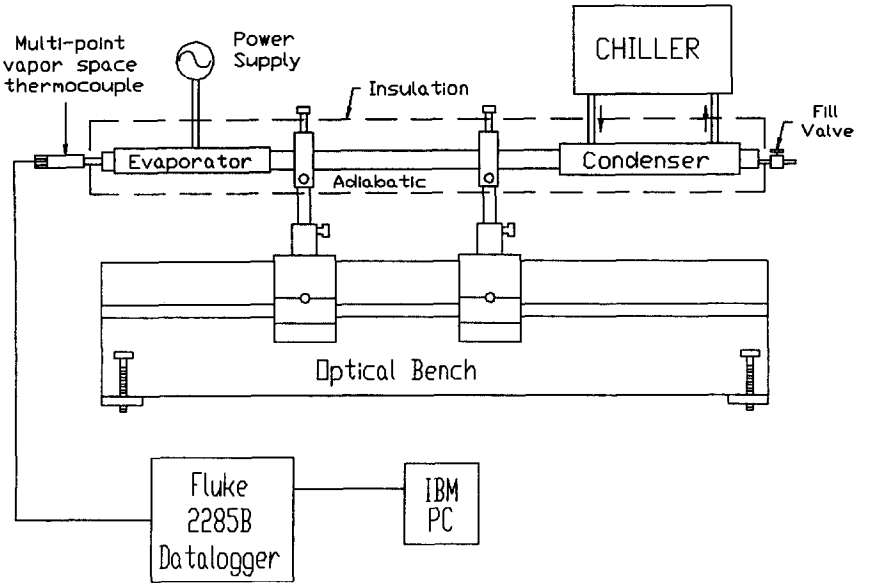

FIG. 1. Experimental set-up.

above 150°C. To ensure that the fluid within the heat pipe was frozen before start-up attempts, a history of the wall temperatures was taken for at least 12 h. Although the gravitational environment can cause pooling of liquid on the bottom side of the pipe prior to freezing, this was considered a minor problem due to the small amount of liquid in the pipe and the capillary forces in the wick, which tend to even out the thickness of the liquid around the circumference of the pipe.

It was necessary that the capillary limit of the pipe be considered due to possible failure other than experimentally controlled criteria. Previous experience with this heat pipe showed that the capillary limit was well over 200 W at 80°C. Since the total heat input was only 20 W, dryout due to the capillary limit was not

Thermocouple locations measured from evaporator end cap

TC #	LOCATION (mm)	TC #	LOCATION (mm)	TC #	LOCATION (mm)
1	125	10	176	19	750
2	403	11	271	20	800
3	554	12	368	21	850
4	634	13	400	22	900
5	834	14	470	23	960
6	990	15	554	24	960
7	10	16	634	25	990
8	52	17	700		
9	118	18	700		

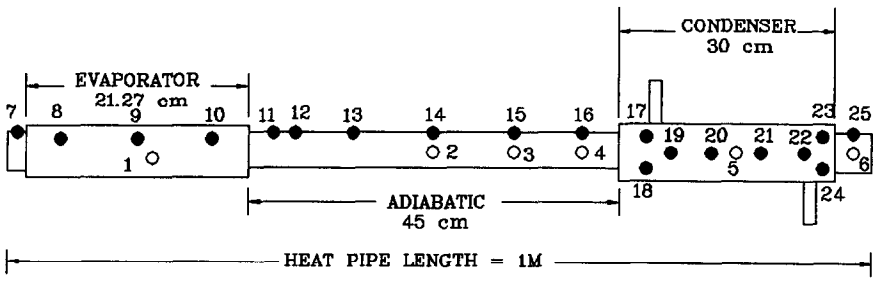

● WALL THERMOCOUPLE
○ VAPOR SPACE THERMOCOUPLE

FIG. 2. Wall and vapor space thermocouple locations.

possible during any of the tests. To verify this point, the following procedure was performed after a failed start-up attempt: before the heat input was stopped, the condenser end was elevated by 70 mm. In all cases, the wall and vapor temperatures became isothermal within 2°C. The heat pipe was then returned to horizontal, but remained isothermal. This proved that the capillary limit was not reached for any cases.

If the test involved a start-up attempt from the frozen state, after the completion of each attempt the entire heat pipe was allowed to thaw until all thermocouples measured at least 21°C, prior to refreezing in preparation for the next test. All tests were duplicated to within ±5% to ensure repeatability. The heat input for Cases 0–5 was 20 W.

The following special procedures were used for the six separate cases reported.

Case 0: Heat pipe tested in a room temperature environment (21°C). Coolant flow began when all condenser wall and vapor temperatures exceeded 28°C. Coolant inlet temperature was 21°C.

Case 1: Heat pipe tested in a freezer (−21 C), frozen for at least 12 h prior to start-up attempt. No coolant flow during any part of the test.

Case 2: Heat pipe tested in a room temperature environment (21°C) after being in a freezer (−21°C) for at least 12 h prior to start-up attempt. Heat applied immediately after heat pipe was removed from freezer. Coolant flow began when condenser temperatures were above 28°C. Coolant inlet temperature was 21°C.

Case 3: Heat pipe tested in a room temperature environment (21°C), frozen completely by −15°C coolant flowing through the condenser. Heat applied and coolant flow halted immediately after entire heat pipe reached −10°C. Coolant flow started again when condenser temperatures were above 28°C. Coolant inlet temperature was 21°C after condenser temperatures reached 28°C.

Case 4: Heat pipe operating at steady state at 35–40°C in a room temperature environment (21°C); −15°C coolant suddenly cycled through condenser for freeze-out.

Case 5: Heat pipe tested in a room temperature environment (21°C) after being frozen in a freezer (−21 C). Heat applied immediately after heat pipe was removed from freezer until temperature difference between any two vapor thermocouples exceeded 3°C. Heat input ceased until all vapor temperature differences were less than 1°C. Process repeated as necessary. Coolant flow not begun until condenser temperatures were greater than 28°C. Coolant inlet temperature was 21°C.

NUMERICAL SIMULATION OF FROZEN START-UP IN THE EARLY STAGES

The heat pipe is a complex system which involves many heat transfer and fluid flow phenomena, such as heat conduction in the wall and wick, melting of the working fluid in the wick, evaporation and condensation at the liquid–vapor interface, liquid flow in the porous wick, and compressible vapor flow in the core. It is therefore very difficult to obtain a generalized analytical solution for the behavior of heat pipes. In recent years, researchers have concentrated on the numerical analysis of the transient heat pipe operation. These include Chang and Colwell [4], Costello *et al.* [5], Hall and Doster [6, 7], Seo and El-Genk [8], Bowman and Hitchcock [9], Jang *et al.* [10, 11], and Cao and Faghri [12]. The numerical models involve different assumptions and are at different stages of development. However, most of these models assume that the working fluid in the wick is completely thawed, and only involve the transient response to a power load with the assumption of continuous vapor flow, except those by Costello *et al.* [5], Hall and Doster [6, 7] and Jang *et al.* [10, 11]. The model of Jang *et al.* [11] may be one of the most comprehensive mathematical models of heat pipe start-up from the frozen state to date. Different start-up periods were described and the general mathematical formulation for each period was given. The emphasis of the present paper is on the early stages of heat pipe start-up from the frozen state.

For a low-temperature heat pipe, experimental results of successful start-up from the frozen state are very rare. Unlike high-temperature heat pipes, experimental results show that the heat pipe immediately becomes active where the ice is melted, but there is still a large temperature gradient in the axial direction. The heat input at the evaporator should be low enough to return a sufficient amount of condensate to the evaporator for successful start-up. The general mathematical simulation model developed by Jang *et al.* [11] included all the physical phenomena at all stages. However, the heat source in the evaporator section did not take into account the additional heat capacity of the material surrounding the evaporator in an actual experiment, such as heater clamps and insulation. In the present study, the model of Jang *et al.* [11] was simplified to examine only the early stages of start-up and to include the additional heat capacity of the material covering the heater in the evaporator section. The present experimental results for two different heat inputs under the conditions corresponding to Case 1 were compared with the numerical simulation model. To the author's knowledge, this is the first effort to compare a numerical simulation model with experimental frozen start-up temperature profiles in the early stages.

The liquid density of the working fluid is much greater than that of the vapor, so the liquid velocity in the wick structure is small. In addition, since the wick is very thin, it is assumed that the effect of the liquid flow in the wick structure is negligible. Thus, the heat transport through the wick structure and working substance is by conduction only, but the phase change of the working substance from solid to liquid is considered. It is also assumed that the wick

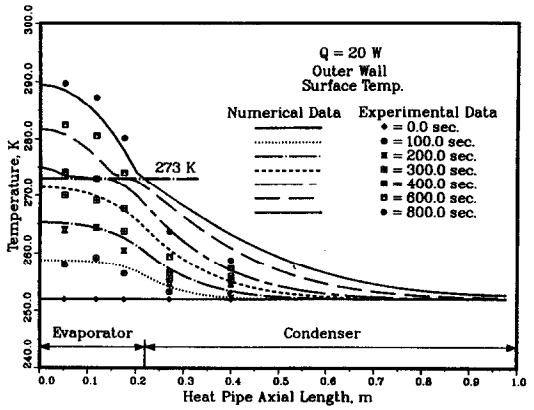

FIG. 3. Comparison of numerical and experimental wall temperature profiles for Case 1 with 20 W.

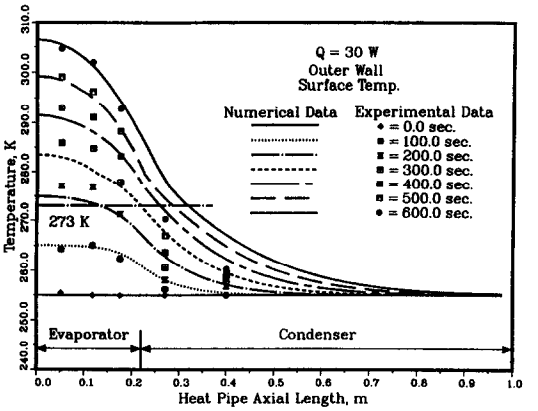

FIG. 4. Comparison of numerical and experimental wall temperature profiles for Case 1 with 30 W.

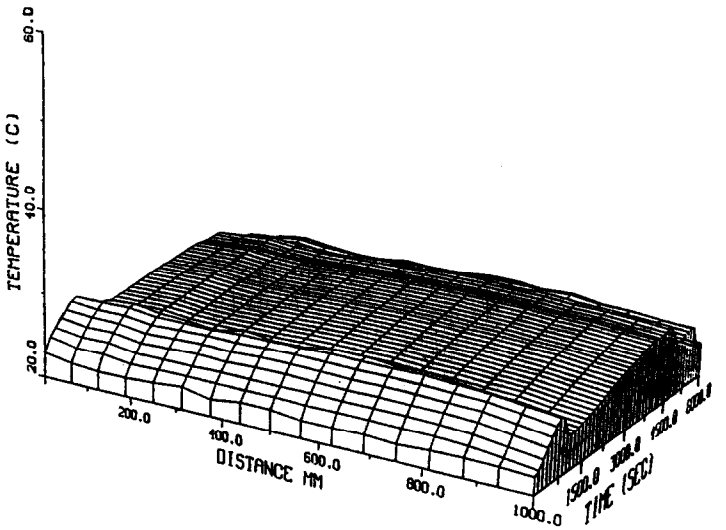

FIG. 5(a). Axial wall temperature profile vs time for Case 0 (baseline).

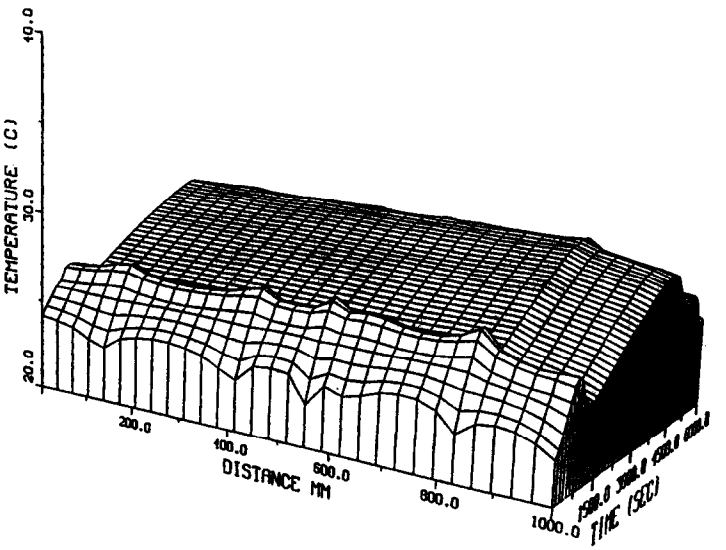

FIG. 5(b). Axial vapor temperature profile vs time for Case 0 (baseline).

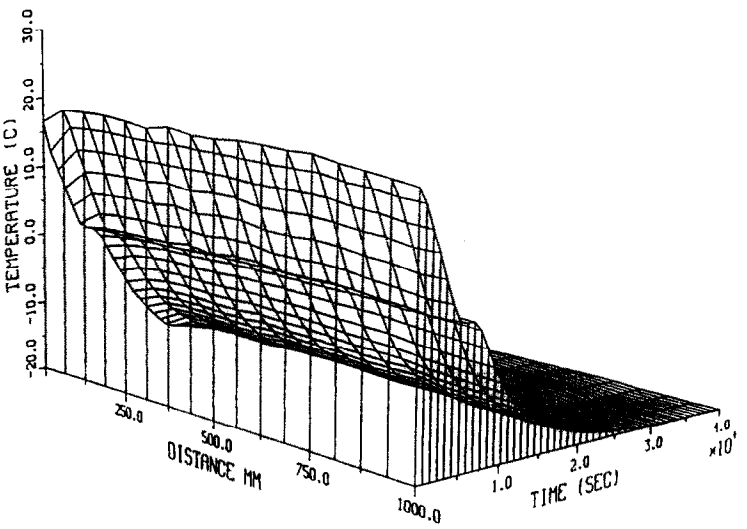

FIG. 6(a). Axial wall temperature profile vs time during freezing in −21°C environment for Case 1.

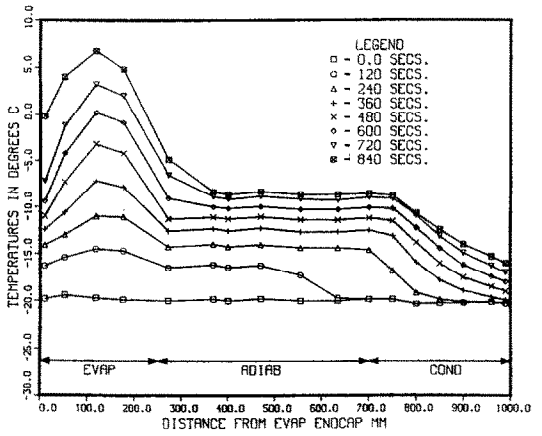

FIG. 6(b). Axial wall temperature profile over time for frozen start-up in −21°C environment for Case 1.

structure is saturated by the working substance. Under these assumptions, the same governing equation is applicable to the heat pipe wall and the wick structure by using the respective properties for each region

$$(\rho c_p)_i \frac{\partial T_i}{\partial t} = \frac{1}{r}\frac{\partial}{\partial r}\left(rK_i \frac{\partial T_i}{\partial r}\right) + \frac{\partial}{\partial x}\left(K_i \frac{\partial T_i}{\partial x}\right) \quad (1)$$

$$i = \begin{cases} \text{w} & \text{for wall region} \\ \text{se} & \text{for solid region} \\ \text{me} & \text{for mushy region} \\ \text{le} & \text{for liquid region.} \end{cases}$$

The expression of $(\rho c_p)_i$ for each region is given as follows:

$$(\rho c_p)_i = \begin{cases} (\rho c_p)_\text{w} & \text{for wall region} \\ \varepsilon(\rho c_p)_\text{fs} + (1-\varepsilon)(\rho c_p)_\text{s} & \text{for solid region in the wick} \\ \varepsilon H_\text{sf}\delta(T - T_\text{m}) + (1-\varepsilon)(\rho c_p)_\text{s} & \text{for mushy region in the wick} \\ \varepsilon(\rho c_p)_\text{fl} + (1-\varepsilon)(\rho c_p)_\text{s} & \text{for liquid region in the wick.} \end{cases} \quad (2)$$

When the effective thermal conductivity for the wick region is calculated by using the expression given by Chang [13], the thermal conductivity for the working substance is substituted by that of the solid, liquid, or the average value of the solid and liquid, corresponding to the solid, liquid, or mushy region, respectively.

The initial condition is

$$T_i(r, x, 0) = T_0. \quad (3)$$

The outer surface of the evaporator section of the experimental heat pipe is surrounded by the heater, a layer of cork, and a copper clamp. An insulation blanket surrounds the outer surface of the copper clamp. The thickness of the heat pipe wall and wick structure is 0.245×10^{-2} m. The thickness of the heater, cork, and copper clamp is 0.546×10^{-2} m. Initially, a uniform temperature of −21°C (252 K) for the wick, wall, heater, cork, and copper clamp is assumed. When the heat input is begun, the heat is actually used to increase the temperature of the heater, cork, and copper clamp as well as the heat pipe wall and wick. Also, there may be some heat loss through the insulation, and the end cap of the evaporator absorbs some heat. In the present numerical model, the presence of the heater, cork, and copper clamp is taken into account. The lumped-mass method is used such that the effective volumetric heat capacity in the evaporator section is evaluated as follows:

$$(\rho c_p)_\text{eff} = \frac{1}{V_\text{w}}[V_\text{w}(\rho c_p)_\text{w} + V_\text{h}(\rho c_p)_\text{h} + V_\text{ck}(\rho c_p)_\text{ck} + V_\text{cc}(\rho c_p)_\text{cc}] \quad (4)$$

where V is the volume of each region, ρ is the density, and c_p is the specific heat. Subscripts w, h, ck, and cc denote the heat pipe wall, heater, cork, and copper clamp, respectively.

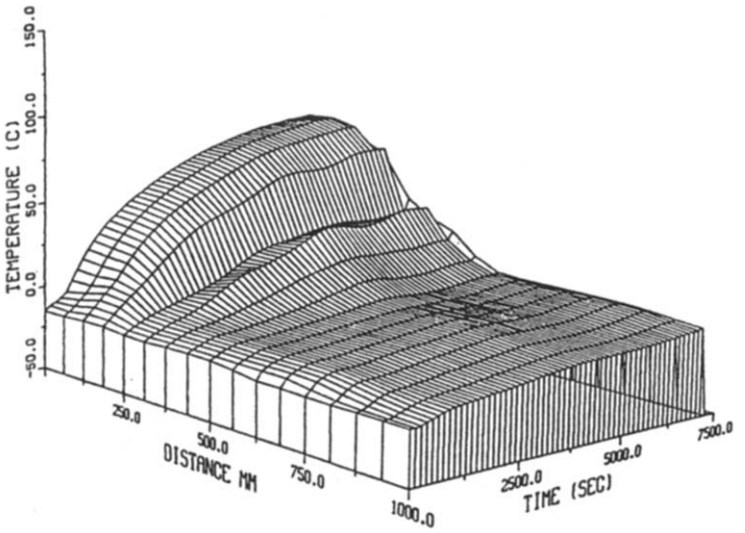

FIG. 7(a). Axial wall temperature profile vs time for frozen start-up in −21°C environment for Case 1.

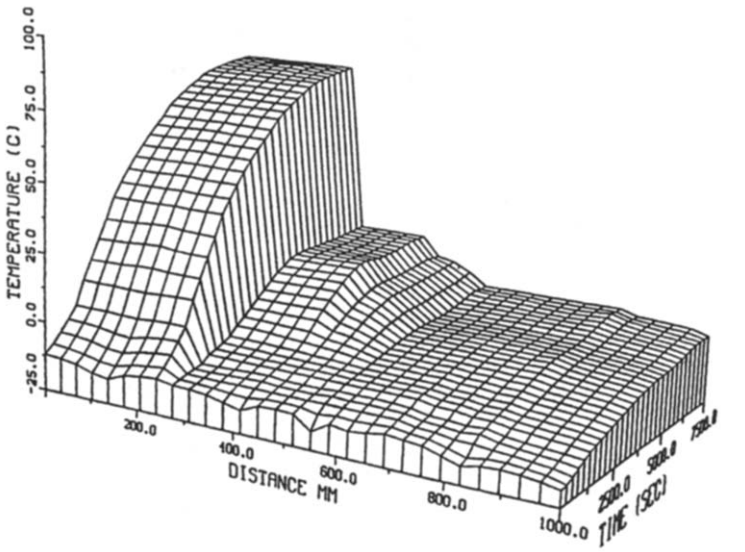

FIG. 7(b). Axial vapor temperature profile vs time for frozen start-up in −21°C environment for Case 1.

The coupling conditions at the liquid–solid interface are

$$T_{se} = T_{le} = T_m \tag{5}$$

$$K_{se}\frac{\partial T_{se}}{\partial n} - K_{le}\frac{\partial T_{le}}{\partial n} = \varepsilon H_{sl}\frac{dS}{dt}. \tag{6}$$

The boundary conditions at the ends of the heat pipe are

$$\frac{\partial T_i}{\partial x} = 0. \tag{7}$$

Based on the continuity of the heat flux and temperature between the heat pipe wall and the wick structure, the boundary conditions are

$$T_i = T_w \tag{8}$$

$$K_i\frac{\partial T_i}{\partial r} = K_w\frac{\partial T_w}{\partial r}. \tag{9}$$

In the first and second periods [11], free molecular flow is prevalent in the vapor space so that the boundary condition at the liquid–vapor interface is

$$\frac{\partial T_i}{\partial r} = 0. \tag{10}$$

The well-known alternating direction implicit (ADI) method is used for the heat pipe wall and wick, and the phase change of the working substance during start-up is modeled by using the equivalent heat

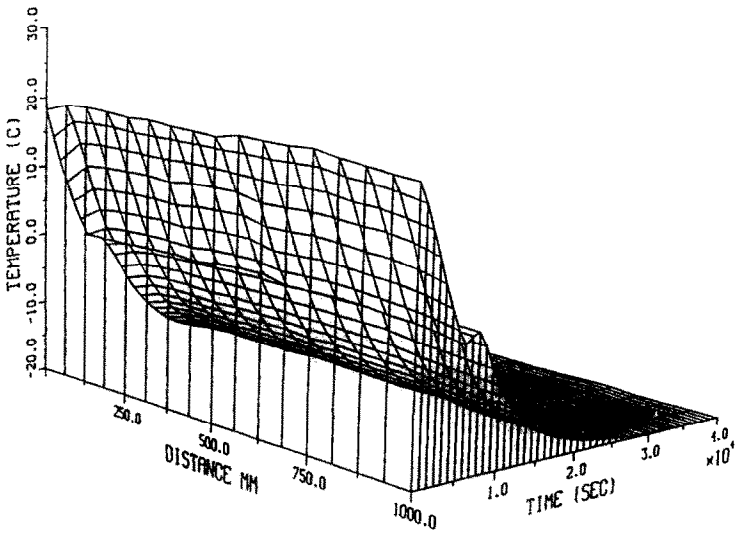

FIG. 8(a). Axial wall temperature profile vs time during freezing in −21 °C environment for Case 2.

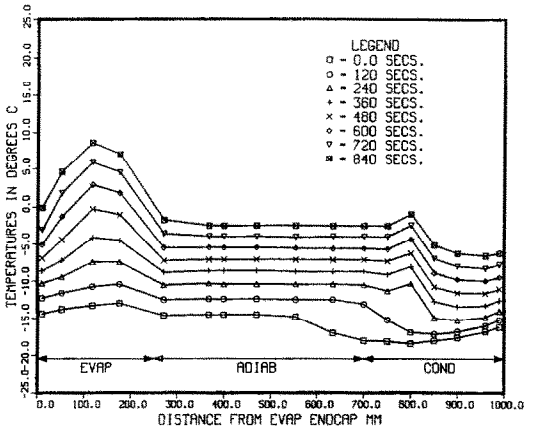

FIG. 8(b). Axial wall temperature profile over time for frozen start-up in 21°C environment for Case 2.

capacity method [14]. This method approximates the rapid change of the heat capacity over the phase-change temperature range, which is an artificially defined finite temperature range, ΔT, instead of using the Dirac function. Thus, equation (2) can be expressed as follows:

$$(\rho c_p)_t = \begin{cases} (\rho c_p)_w & \text{for wall region} \\ \varepsilon(\rho c_p)_{fs} + (1-\varepsilon)(\rho c_p)_s & \text{for solid region} \\ \varepsilon\left[\dfrac{(\rho c_p)_{fs} + (\rho c_p)_{fl}}{2} + \dfrac{H_{sl}}{2\Delta T}\right] + (1-\varepsilon)(\rho c_p)_s & \text{for mushy region} \\ \varepsilon(\rho c_p)_{fl} + (1-\varepsilon)(\rho c_p)_s & \text{for liquid region.} \end{cases} \quad (11)$$

In the numerical calculation, this property is evaluated based on the nodal temperatures.

Figure 3 shows the numerical outer wall temperature prediction along the heat pipe and comparison with experimental data for various times for a heat input of 20 W, corresponding to Case 1. As heat was added in the evaporator, the temperature in the evaporator increased with time, and at approximately 400 s the working fluid in the evaporator was in the liquid state. However, the temperature in the end of the condenser did not change from the initial temperature. If the heat input is continued at the evaporator, heating and vaporization of liquid may occur at the evaporator section. However, the working substance in the condenser would still be in the solid state. Figure 4 shows the wall temperature profile for a heat input of 30 W, corresponding to Case 1. As the heat was added in the evaporator section, the temperature in the evaporator again increased with time, and at approximately 300 s the working fluid in the evaporator was in the liquid state. Again, the working fluid in the condenser remained completely frozen. Therefore, the heat input in the evaporator should be small to prevent dryout of the wick structure in the evaporator while the working substance in the rest of the heat pipe is melted.

EXPERIMENTAL RESULTS AND DISCUSSION

Case 0 was conducted to obtain a baseline for comparison of the normal and frozen start-up data. Wall and vapor temperature data along the length of the heat pipe for a normal start-up were recorded for 2 h, as presented in Fig. 5. The heat pipe remained nearly isothermal throughout the experiment. When the flow of coolant began, an immediate drop in the vapor temperature occurred over the entire heat pipe. Subsequent adjustments of coolant temperature resulted in similar changes in the temperature, which appear

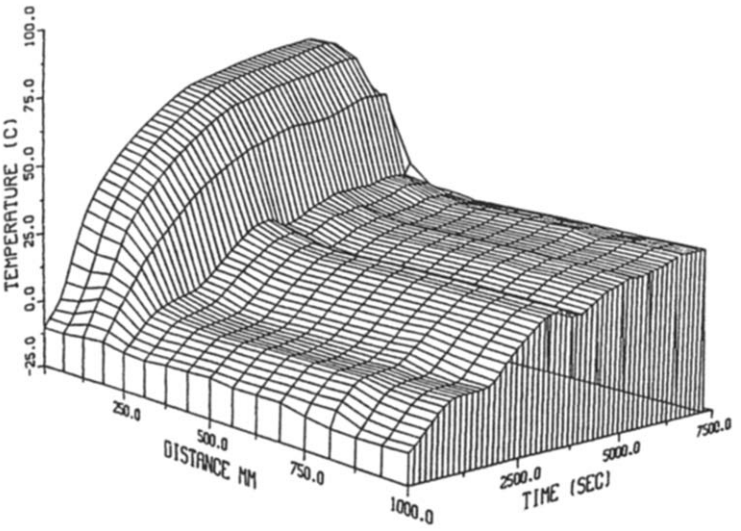

FIG. 9(a). Axial wall temperature profile vs time for frozen start-up in 21°C environment for Case 2.

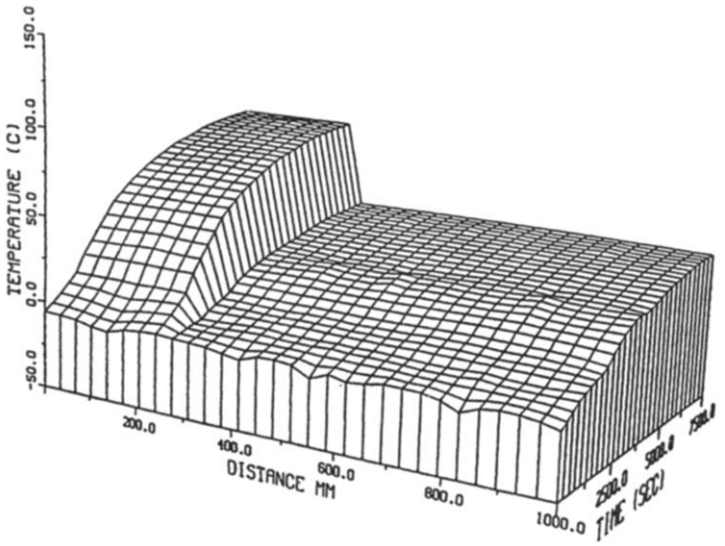

FIG. 9(b). Axial vapor temperature profile vs time for frozen start-up in 21°C environment for Case 2.

as uniform dips in the surface of data points over time. At no time did the wall or vapor temperatures along the pipe, before or after the flow of coolant had begun, vary by more than 2°C.

The start-up behavior of the heat pipe in a subfreezing environment (Case 1) is presented in Figs. 6 and 7. To ensure that the working fluid was completely frozen, the wall temperatures were recorded during the 12 h prior to the start-up attempt, as shown in Fig. 6(a). The wall temperatures remained at 0°C while the working fluid changed phase from liquid to solid, as expected. Figure 6(b) presents the axial wall temperatures in the early period during the start-up attempt. At the beginning of the test, the wall temperature was uniform across the pipe length. At 120 s, the wall temperature in the evaporator and part of the adiabatic section increased by nearly 5°C, while those in the rest of the adiabatic section and condenser remained at the initial temperature. This demonstrated that the frozen start-up behavior of this copper/water heat pipe was frontal in nature, which is similar to that of high-temperature heat pipes. This frontal start-up mode has a very short transient period, as shown by the increase in the condenser end cap temperature between 360 and 480 s. Even though no coolant flowed through the condenser, heat was transferred to the coolant by natural convection, as shown by the decrease in the wall temperature in the condenser section.

In examining the temperatures in the evaporator section, one finds that the evaporator end cap temperature is within 1°C of that in the adiabatic section until 600 s. After this time, the end cap temperature rose very quickly while the adiabatic temperatures

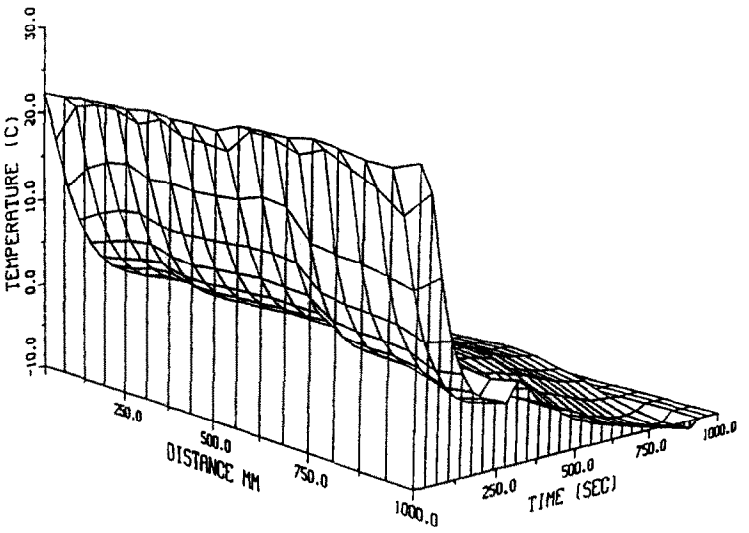

FIG. 10(a). Axial wall temperature profile vs time during freezing with chiller for Case 3.

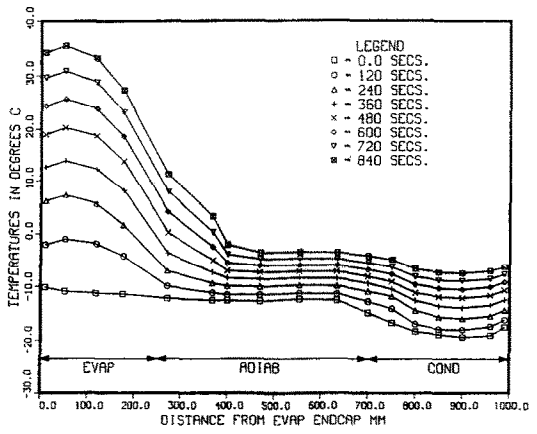

FIG. 10(b). Axial wall temperature profile over time for frozen start-up for Case 3.

changed slowly. This shows that from 0 to 600 s, the frozen working fluid melted, vaporized, and traveled toward the condenser as during normal operation. After 600 s, most of the working fluid in the evaporator section had evaporated. Since the working fluid in the adiabatic section was still frozen, the wick in the evaporator was not replenished with condensate, which resulted in dryout. This is shown in Fig. 7 over 2 h. The wall and vapor temperatures increased and then leveled off, but the temperature difference from one end to the other was greater than 50°C. In comparing this to the baseline experiment where the temperature difference from end to end was only 2°C, it is obvious that this test resulted in start-up failure.

The results of Case 2 are presented in Figs. 8 and 9, where the heat pipe was placed in the freezer for 12 h at −21°C, and then removed for testing at room temperature (21°C). The freezing history is shown in Fig. 8(a) and the start-up attempt in the early period is given in Fig. 8(b).

In comparing Fig. 8(b) with Fig. 6(b), one can see the effect of the ambient temperature change in the wall temperatures at the beginning and end of the condenser section. At these locations, the wall temperature was higher when in the room temperature environment due to heat conduction through the end caps of the calorimeter from the ambient. Despite the change in the wall temperature profile, the frontal start-up mode was still apparent in this case, which ended between 120 and 240 s. Dryout began between 720 and 840 s, which was later than Case 1 due to the additional melting of the working fluid from the ambient heat. This additional melting, however, was insufficient to avoid start-up failure.

Figures 9(a) and (b) present the wall and vapor temperatures, respectively, for Case 2 over 2 h. The results are similar to Case 1 in that the temperatures leveled off with a large overall temperature drop across the heat pipe compared to the baseline. In contrast to Case 1, however, the wall and vapor temperatures in the adiabatic and condenser sections were well above 0°C, again demonstrating the effect of the ambient environment. Even though the heat pipe was well insulated, heat can pass from the environment to the pipe and vice versa. Again, this additional heat input from the ambient did not prevent start-up failure.

In Case 3, the working fluid was frozen in the room temperature environment by supplying the calorimeter with −15°C coolant. While the freezing history (Fig. 10(a)) was very similar to those of Cases 1 and 2, the initial period of the start-up attempt (Fig. 10(b)) was significantly different. Dryout began immediately after the heat was applied. This sudden dryout was due to the method of freezing the working fluid. Starting from the ambient conditions, the condenser section was cooled below the freezing point, but the evaporator section was above freezing. During this period, liquid in the evaporator continued to evap-

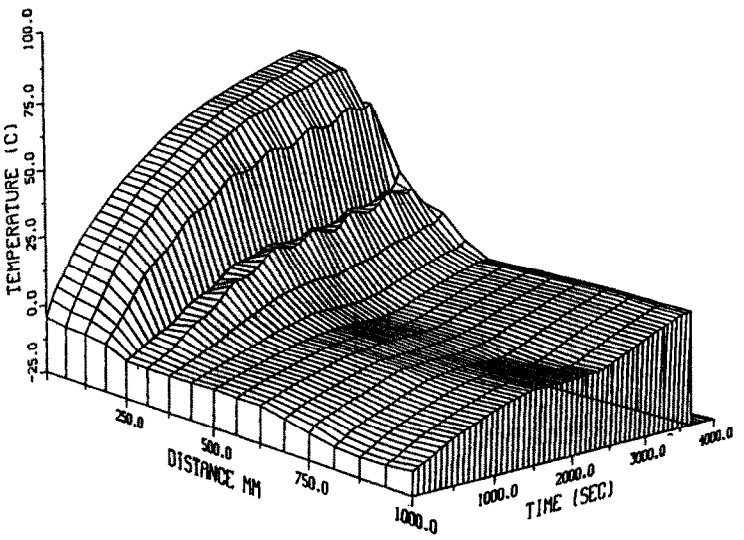

FIG. 11(a). Axial wall temperature profile vs time for frozen start-up for Case 3.

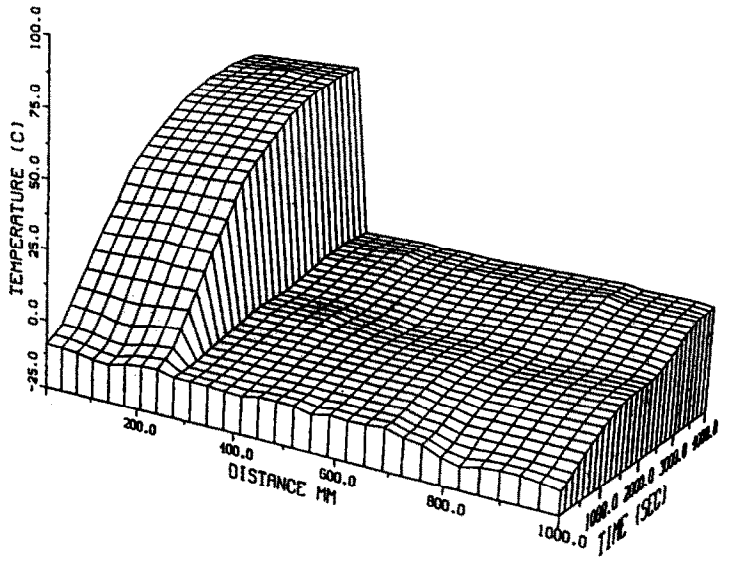

FIG. 11(b). Axial vapor temperature profile vs time for frozen start-up for Case 3.

orate and travel to the condenser section, where it condensed and also froze. This continued until the liquid in the adiabatic section and finally the evaporator section froze. However, a significant portion of working fluid that would normally be in the evaporator section was now frozen in the condenser section, which led to early dryout. Figure 11 presents the wall and vapor temperatures over several hours, which again demonstrate an unsuccessful start-up attempt for Case 3.

Wall and vapor temperature data for Case 4 are given in Fig. 12. The heat pipe was started normally at room temperature, run at a steady-state temperature of 35–40°C for 30 min with a coolant temperature of 21°C, and then the coolant temperature was decreased from 21°C to −15°C. The wall and vapor temperatures in the condenser section dropped monotonically over the 2 h test, but the evaporator section temperatures first decreased and then increased. This indicated that the working fluid in the condenser froze and collected the working fluid from the evaporator section, which then dried out.

The Case 5 test started by freezing the heat pipe in the −21°C environment, placing it in room temperature (21°C) conditions, and then starting the heat by pulsing the heat input on and off. When the vapor temperature difference between any two thermocouples exceeded 3°C, the heat input was ceased. When the vapor temperature differences among all of the thermocouples was less than 1°C, the heat input

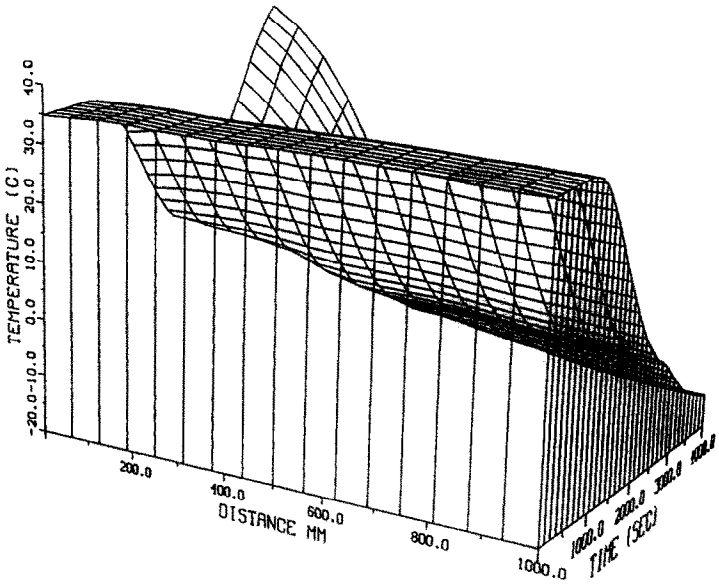

FIG. 12(a). Axial wall temperature profile vs time during freezing while operating in 21°C environment for Case 4.

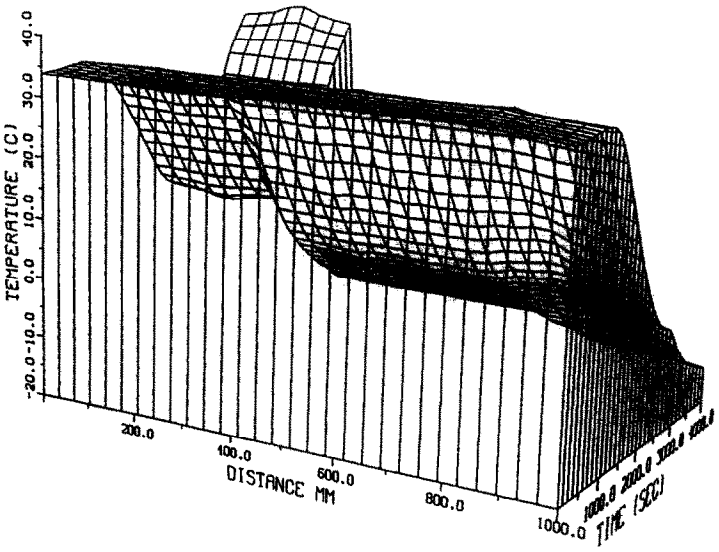

FIG. 12(b). Axial vapor temperature profile vs time during freezing while operating in 21°C environment for Case 4.

was started again. Since the baseline case gave an overall temperature drop of 2°C, the 3°C criterion was chosen as the onset of dryout. The 1°C criterion was chosen due to the uncertainties of the thermocouple readings. Figure 13(a) presents the initial start-up behavior. From 0.0 to 120 s, heat was input to the evaporator, which caused the onset of dryout. After 120 s, the heat input was stopped, resulting in the temperatures across the pipe becoming more uniform, as seen in the 240 and 360 s profiles. Between 360 and 480 s, the heat was again applied, causing another sudden jump in the evaporator temperatures. Between 480 and 600 s the heat was again discontinued, which allowed the evaporator temperatures to decrease and the adiabatic and condenser section temperatures to increase. The frontal start-up behavior in this case can be seen in the curves of 120, 240, and 360 s, in which the temperature gradient was very steep at first, and then quickly became flatter.

Using this method, six pulses were required for start-up, which all occurred at subfreezing temperatures. Temporarily stopping the heat input to the evaporator allowed time for the working fluid in the section immediately adjacent to the hot zone to melt and rewet the wick. When the vapor temperature equalized, another pulse could be applied. It is note-

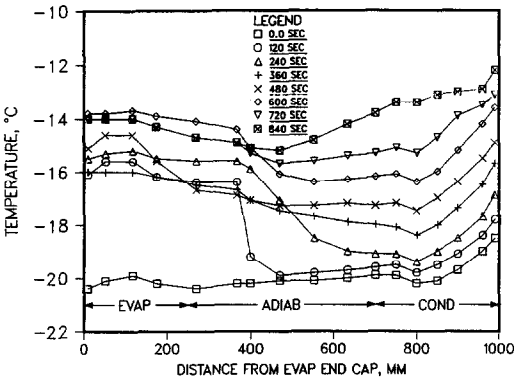

FIG. 13(a). Axial wall temperature profile over time for frozen start-up with pulsed heat input for Case 5.

worthy that these pulses were no longer required above −5°C. As seen in Figs. 13(b) and (c), nearly isothermal start-up was achieved. Steady-state operation was verified for 2 h afterwards.

CONCLUSIONS

The frozen start-up behavior of a copper/water heat pipe has been experimentally and numerically investigated. A method of starting a frozen heat pipe was demonstrated experimentally, which involved pulsing the heat input on and off. A numerical simulation model predicted start-up failure with excellent agreement with the experimental data.

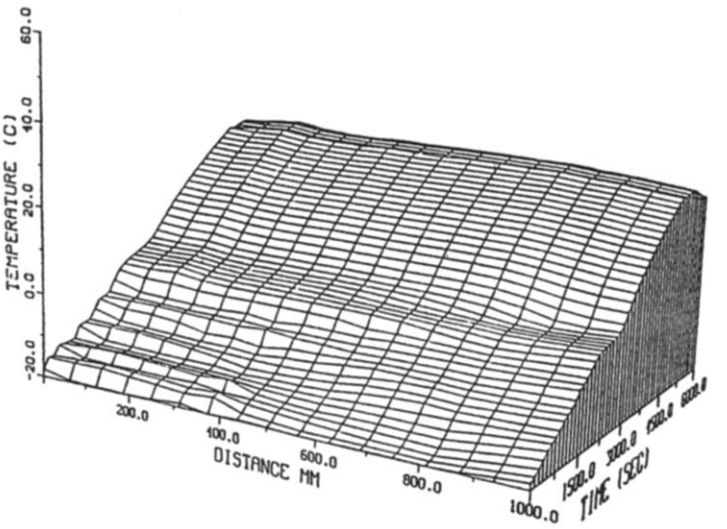

FIG. 13(b). Axial wall temperature profile vs time for frozen start-up with pulsed heat input for Case 5.

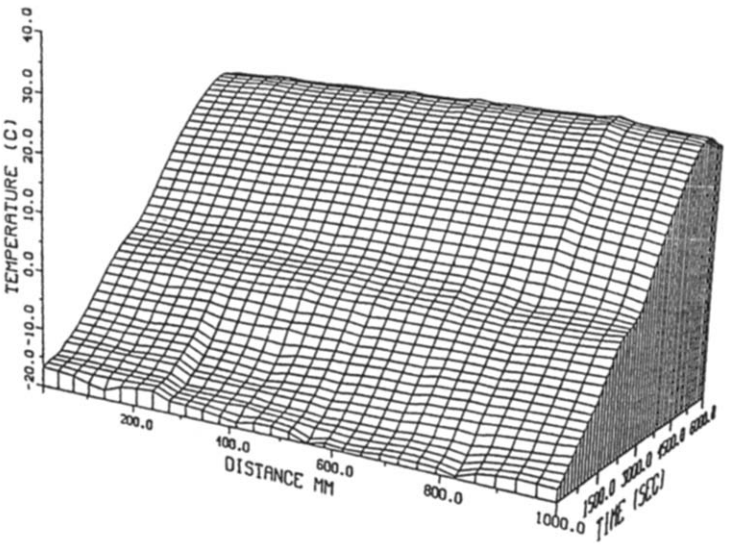

FIG. 13(c). Axial vapor temperature profile vs time for frozen start-up with pulsed heat input for Case 5.

Acknowledgements—This project was sponsored by the NASA Lewis Research Center and the U.S. Air Force. The assistance from Mr Dan Mitchell, Ms Lynne Browne, Mr Scott Thomas and Dr Jong Hoon Jang is acknowledged.

REFERENCES

1. L. G. Neal, An analytical and experimental study of heat pipes, TRW Systems Report 999000-6114-R000 (1987).
2. J. E. Deverall and J. E. Kemme, Sonic limitations and startup problems of heat pipes, Los Alamos Report (1970).
3. T. P. Cotter *et al.*, Heat pipe startup dynamics, *Proc. Thermionics Conversion Specialist Conf.* (1967).
4. W. S. Chang and G. T. Colwell, Mathematical modeling of the transient operating characteristics of a low-temperature heat pipe, *Numer. Heat Transfer* **8**, 169–186 (1985).
5. F. A. Costello *et al.*, Detailed transient model of a liquid-metal heat pipe, *Trans. 4th Symp. on Space Nuclear Power Systems*, CONF-870102-Summs, pp. 393–402 (1987).
6. M. L. Hall and J. M. Doster, Transient thermohydraulic heat pipe modeling, *Trans. 4th Symp. on Space Nuclear Power Systems*, pp. 407–410 (1987).
7. M. L. Hall and J. M. Doster, A sensitivity study of the effects of evaporation/condensation accommodation coefficients on transient heat pipe modeling, *Int. J. Heat Mass Transfer* **33**, 465–481 (1990).
8. J. T. Seo and M. S. El-Genk, A transient model for liquid-metal heat pipes, *Proc. 5th Symp. on Space Nuclear Power Systems* (1988).
9. J. Bowman and J. Hitchcock, Transient compressible heat pipe vapor dynamics, *Proc. 25th ASME National Heat Transfer Conf.*, Vol. 1, pp. 329–338 (1988).
10. J. H. Jang, A. Faghri and W. S. Chang, Analysis of the transient compressible vapor flow in heat pipes, *Int. J. Heat Mass Transfer* **34**, 2029–2037 (1991).
11. J. H. Jang, A. Faghri, W. S. Chang and E. T. Mahefkey, Mathematical modeling and analysis of heat pipe start-up from the frozen state, *ASME J. Heat Transfer* **112**, 586–594 (1990).
12. Y. Cao and A. Faghri, A transient two-dimensional compressible analysis for high temperature heat pipes with a pulsed heat input, *Numer. Heat Transfer* **18**, 483–502 (1990).
13. W. S. Chang, Effective thermal conductivity of wire screens, *24th ASME/AIChE National Heat Transfer Conf.* (1987).
14. J. S. Hsiao, An efficient algorithm for finite difference analysis of heat transfer with melting and solidification, ASME Paper No. 84-WA/HT-42 (1984).

DEMARRAGE DE CALODUCS GELES ET FONCTIONNANT A BASSE TEMPERATURE

Résumé—Le démarrage et le fonctionnement ultérieur d'un caloduc à basse température exige que la phase liquide du fluide de travail soit continûment pompé par action capillaire de la mèche vers l'évaporateur. Si le caloduc a été dans une ambiance à température inférieure au point de gel du fluide avant le démarrage, le fluide gelé dans le condenseur et les régions adiabatiques peuvent empêcher l'écoulement initial vers l'évaporateur et provoquent le séchage de celui-ci avant que le fluide soit en phase liquide. On examine ici les profils variables de température de paroi et de vapeur le long de l'axe d'un caloduc à basse température pendant le démarrage à partir de l'état gelé. En outre, le profil de température de paroi au démarrage, déterminé expérimentalement, est comparé à celui donné par un modèle numérique bidimensionnel à changement de phase. On présente une méthode de démarrage favorable utilisant une alimentation énergétique pulsée.

ANFAHRVERHALTEN EINES NIEDERTEMPERATUR-WÄRMEROHRS MIT EINGEFRORENEM WÄRMETRÄGERMEDIUM

Zusammenfassung—Während der Anfahrphase und des kontinuierlichen Betriebs eines Niedertemperatur-Wärmerohrs ist ein kontinuierlicher Rücktransport des Arbeitsfluids in flüssiger Form durch die Kapillarwirkung des Dochtes erforderlich. Sofern vor der Inbetriebnahme das Wärmerohr Temperaturen ausgesetzt ist, die unterhalb des Gefrierpunkts des Arbeitsfluids liegen, wird durch das gefrorene Medium in der Kondensations- und Transportzone ein Rücktransport zur Verdampfungszone unterbunden. In der Folge trocknet die Verdampfungszone aus, ehe das gesamte Arbeitsfluid verflüssigt ist. In der vorliegenden Arbeit wird die zeitliche Entwicklung der axialen Wand- und Dampftemperaturprofile in einem Niedertemperatur-Wärmerohr während der Anfahrphase vom gefrorenen Zustand untersucht. Zusätzlich wird auch das Ausfrieren während des normalen Betriebs durch entsprechende Kühlung des Kondensators betrachtet. Die Meßergebnisse für die Temperaturprofile an der Wand während der Anfahrphase werden mit Rechenergebnissen aufgrund eines numerischen zweidimensionalen Phasenänderungsmodells verglichen. Abschließend wird ein erfolgreiches Anfahrverfahren vorgestellt, das auf einer gepulsten Wärmezufuhr beruht.

ПОВЕДЕНИЕ НИЗКОТЕМПЕРАТУРНЫХ ТЕПЛОВЫХ ТРУБ ПРИ ЗАПУСКЕ ИЗ ЗАМОРОЖЕННОГО СОСТОЯНИЯ

Аннотация—Запуск и последующая работа низкотемпературной тепловой трубы требуют непрерывной откачки жидкой фазы рабочей среды к испарителю за счет капиллярного действия фитиля. Если тепловая труба перед запуском находится в среде с температурой ниже точки замерзания рабочей жидкости, замерзшая жидкость может подавить начальное течение к испарителю, что приведет к кризису теплопереноса в испарителе до того, как вся рабочая среда перейдет в жидкую фазу. Исследуются нестационарные температурные профили стенки и пара вдоль оси низкотемпературной тепловой трубы при запуске из замороженного состояния, а также вымораживание при работе в нормальных условиях посредством пропускания через конденсатор жидкости с температурой ниже точки замерзания. Кроме того, экспериментальный нестационарный профиль температур стенки при запуске из замороженного состояния сравнивается с результатами, которые дает двумерная численная модель фазового перехода. Описывается метод запуска с использованием импульсного подвода мощности.